



#### Contents

- 1 Abstract
- 1 Introduction
- 3 Methods
- 5 Results
- 6 Acknowledgments
- 6 References

#### Keywords

International Ocean Discovery Program, IODP, *JOIDES Resolution*, Expedition 362, Expedition 353, Sumatra Subduction Zone, Indian Monsoon Rainfall, Site U1443, Site U1444, Site U1445, Site U1446, Site U1447, Site U1448, Site U1480, Site U1481

#### Supplementary material

#### References (RIS)

#### MS 362-207

Received 10 August 2022  
Accepted 21 October 2022  
Published 4 April 2023

# Data report: chemical compositions of marine tephra layers in the Indian Ocean, IODP Expeditions 353 and 362<sup>1</sup>

Steffen Kutterolf,<sup>2</sup> Julie C. Schindlbeck-Belo,<sup>2</sup> Katharina Pank,<sup>2</sup> Kuo-Lung Wang,<sup>3,4</sup> and Hao-Yang Lee<sup>3</sup>

<sup>1</sup> Kutterolf, S., Schindlbeck-Belo, J.C., Pank, K., Wang, K.-L., and Lee, H.-Y., 2023. Data report: chemical compositions of marine tephra layers in the Indian Ocean, IODP Expeditions 353 and 362. In McNeill, L.C., Dugan, B., Petronotis, K.E., and the Expedition 362 Scientists, Sumatra Subduction Zone. *Proceedings of the International Ocean Discovery Program*, 362: College Station, TX (International Ocean Discovery Program). <https://doi.org/10.14379/iodp.proc.362.207.2023>

<sup>2</sup> GEOMAR Helmholtz Centre for Ocean Research, Kiel, Germany. Correspondence author: [skutterolf@geomar.de](mailto:skutterolf@geomar.de)

<sup>3</sup> Institute of Earth Sciences, Academia Sinica, Taiwan

<sup>4</sup> Department of Geosciences, National Taiwan University, Taiwan

## Abstract

We report on a total of 310 samples from marine sediments drilled in the Indian Ocean that were analyzed for glass shard compositions. Samples are mainly from International Ocean Discovery Program Expeditions 353 and 362 but are complemented by samples from Expedition 354; Ocean Drilling Program Legs 183, 121, 120, 119, 116, and 115; and Deep Sea Drilling Project Leg 22. We performed 4327 successful single glass shard analyses with the electron microprobe for major element compositions and conducted 937 successful single analyses with laser ablation-inductively coupled plasma-mass spectrometry (LA-ICP-MS) for trace element compositions on individual glass shards previously measured with the electron microprobe. In total, we were able to measure glass compositions for 254 samples. Of all the samples, 235 can be classified as tephra layers containing pyroclasts as the predominant component in their clast inventory between the 63 and 125  $\mu\text{m}$  grain size fraction, often exceeding 90 vol%. The compositions of the Indian Ocean marine tephtras range from basalt to rhyolite and from basaltic trachyandesite to trachyte and fall into the calc-alkaline, K-rich calc-alkaline, and shoshonitic magmatic series.

## 1. Introduction

International Ocean Discovery Program (IODP) Expedition 362 was initiated to investigate the seismic behavior of the Sumatra subduction zone, which was the location of one of the most devastating earthquakes in human history. The goal of Expedition 362 was to establish initial and progressing properties of the thick, diagenetically overprinted North Sumatran incoming sedimentary section by coring and to determine their role in the shallow seismogenesis and forearc plateau development that led to large earthquakes in the past (McNeill et al., 2017b). On the other hand, the incoming plate, with its thick sediment cover, has been influenced by different spatially and temporally variable sediment fans providing eroded material from the Himalaya Mountain chain. Investigating the sedimentology and climate-dependent and temporal variable sediment properties will help us understand the response of monsoon systems to climate forcing. This goal was also the predominant scientific objective of IODP Expedition 353, during which six sites were drilled in the Bay of Bengal (Clemens et al., 2016).

In addition to the climate driven deposition of Himalayan and Sumatran debris in the hemipelagic and pelagic sediment sequences, traces of large volcanic eruptions have also been incorporated in the sediments in the form of ash layers. Sources for these eruptions are the nearby Sumatra volca-

nic arc, and larger eruptions might derive from the more distant Banda and Java arcs, all together known as the Sunda arc (Figure F1). Other sources are the Philippines, Andaman arc, and island volcanoes in the Indian Ocean. The cores from IODP Expeditions 353 and 362, complemented by cores from IODP Expedition 354; Ocean Drilling Program (ODP) Legs 183, 121, 120, 119, 116, and 115; and Deep Sea Drilling Project (DSDP) Leg 22 provide a long-lasting and Indian Ocean-wide sediment archive spanning the entire Tertiary and Quaternary, where traces of these eruptions can be investigated (Figure F1).

Here we report on major and trace element glass shard compositions of tephra layers from these expeditions. Data of the compositions of discrete layers can be used to evaluate their primary (eruption-related) versus secondary (reworked) origin and to correlate between sites and correlative data from onshore tephra samples. Therefore, the eight drill sites from Expeditions 353 (Indian Monsoon Rainfall) and 362 (Sumatra Subduction Zone) provide the unique opportunity to investigate the history of the highly explosive volcanic activity of the entire Sunda arc and its signal in marine sediments over a time span of about 20 My. As a result, the compositional data provided here will be the base for the upcoming publications to (1) construct a compositional and temporal tephrostratigraphic framework for cores from Expeditions 353 and 362, complemented by Leg 121 Site 758, from the Campanian to recent; (2) correlate tephra layers between the individual holes and sites and determine tephra ages; and (3) extend the tephrostratigraphy to the other DSDP/ODP/IODP cores from the entire Indian Ocean to establish an ocean-wide tephrochronostratigraphy. The combined results of these objectives will provide geochronological and geotechnical information for experiments for other Expedition 353 and 362 scientists and will help to verify age models and sedimentation rates and decipher the provenance of the tephra layers and sediments.

The majority of sampled and investigated potential tephra horizons were retrieved from six sites drilled in the Bay of Bengal during Expedition 353 (Figure F1) (Site U1443 on the Ninetyeast Ridge; Sites U1447 and U1448 in the Andaman Sea; and Sites U1444, U1445, and U1446 in the Bengal Fan). The extended upper Pleistocene to upper Miocene succession consists of greenish gray hemipelagic clays with varying abundances of nannofossils, foraminifers, and biosiliceous

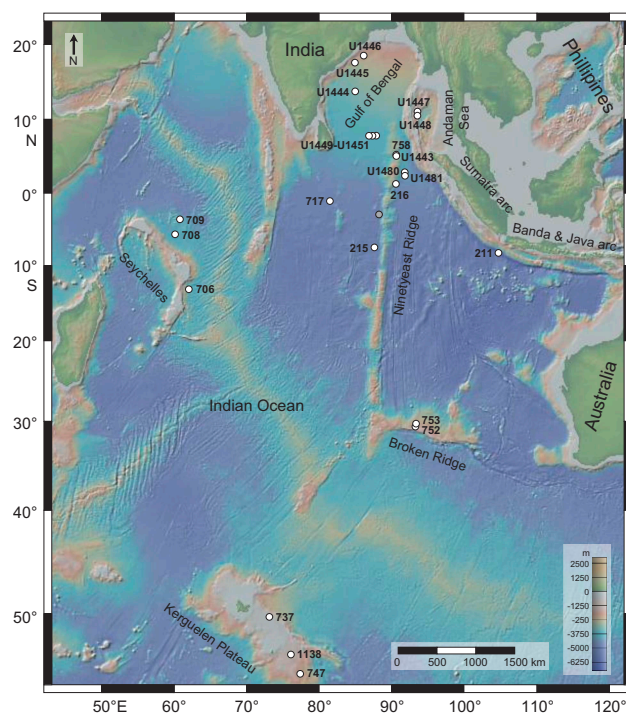


**Figure F1.** Overview map showing the Indian Ocean (<https://www.geomapp.org>; GMRT-Global Multi-Resolution Topography; Ryan et al., 2009) with investigated DSDP, ODP, and IODP drill sites (white circles) of Legs 22, 115, 116, 119, 120, 121, 183, 153 and Expeditions 354 and 362 that were sampled and analyzed for this publication.

components discordantly overlying middle Miocene greenish gray to light greenish gray biosiliceous oozes with varying proportions of clay and nannofossils (Clemens et al., 2016).

Sediments recovered from Site U1443 reveal a range of pelagic and hemipelagic sediments of late Pleistocene to Campanian age, comprising four distinct lithostratigraphic units (Clemens et al., 2016). The upper late Pleistocene–late Miocene part (0–107.80 meters below seafloor [mbsf]) is mainly made of nannofossil oozes with varying proportions of foraminifers, clay, and often occurring discrete ash layers. The deeper part of the sediment succession consists of an increasing amount of chalk with variable contents of authigenic carbonate and foraminifers. The lowermost part comprises a succession of greenish gray marlstones with glauconite of late Campanian age.

Lithologies at Sites U1444–U1446 are either siliciclastic composed of turbidites with intercalated hemipelagic intervals or hemipelagic clays with a significant biogenic component and occasional thin turbidites of late Pleistocene (Holocene?) to late Miocene age, depending on the position within the Bengal Fan (Clemens et al., 2016). This is similar to Expedition 354 Sites U1449–U1451 (France-Lanord et al., 2016), where discrete ash layers from presumably large eruptions are sporadically intercalated within the fan-derived sediments.

During Expedition 362, sediments were recovered to a maximum depth of 1500 mbsf at Sites U1480 and U1481 on the Indian oceanic plate, ~250 km southwest of the subduction zone (Figure F1). A detailed description of the results can be found in the Site U1480 and Site U1481 chapters of the IODP Proceedings volume (McNeill et al., 2017c; McNeill et al., 2017d). The complete sedimentary section is composed of Late Cretaceous to recent deep-marine sedimentary cover, including an upper thick pile (0–1250.3 mbsf) of clastic Nicobar Fan sedimentation containing a range of siliciclastic turbidite deposits from sources in the Himalayan-derived Ganges-Brahmaputra river system, Indo-Burman range/West Burma, and Sunda forearc and arc (McNeill et al., 2017a; McNeill et al., 2017b; Pickering et al., 2020). The lower (1250.35–1349.8 mbsf) sedimentary sequence is dominated by pelagic sedimentation with significantly reduced sediment accumulation rates before calcareous claystones and chalks with intercalated magmatic intrusions (1349.8–1415.3 mbsf) mark the transition into the igneous basement starting at 1415.3 mbsf (McNeill et al., 2017a; McNeill et al., 2017b).

Additionally, we revisited the cores from ODP Legs 183, 121, 120, 119, 116, and 115 and DSDP Leg 22 to complement the tephra inventory of the Indian Ocean (Figure F1). Site 758 (Leg 121) is at the same position as Site U1443 (Expedition 353), whereas Sites 215 and 216 (Leg 22) are located toward the south, on or close to the Ninetyeast Ridge. Site 717 (Leg 116) samples the distal Bengal Fan 700 km south of Sri Lanka, and Site 211 (Leg 22) is positioned close to the Sunda Strait. Sites 706, 708, and 709 (Leg 115) are located in the southeastern part of the Indian Ocean close to the Seychelles, whereas Sites 737, 747, and 1138 (Legs 119, 120, and 183, respectively) and Sites 752 and 753 (Leg 121) were drilled in the central southern part of the Indian Ocean and targeted the Kerguelen Plateau and the Broken Ridge, respectively. All these sites contain a long-lasting (Quaternary and Tertiary) pelagic sedimentation consisting of nannofossil to diatom ooze with some terrestrial influences closer to islands or continents and interbedded traces of volcanic eruptions (Coffin et al., 2000; Peirce et al., 1989; Schlich et al., 1989; Barron et al., 1989; Backman et al., 1988).

## 2. Methods

### 2.1. Core sampling

Shipboard visual core descriptions are used to identify intervals of interest indicating possible discrete ash layers (McNeill et al., 2017b; Clemens et al., 2016; France-Lanord et al., 2016; Shipboard Scientific Party, 1974; Peirce et al., 1989; Cochran et al., 1989; Coffin et al., 2000; Schlich et al., 1989; Barron et al., 1989; Backman et al., 1988). The archive-half sections of the sediment cores were visually described for lithologic and sedimentary features aided by 20× wide-field hand lens and binocular microscope. Visual inspection and smear slide analysis yielded information about variations in lithologic components, color, sedimentary structures, and occasionally drilling disturbances. Lithologic components comprise tephra particles (glass and minerals) as well as various rock fragments and microfossils. Samples of discrete ash layers were taken from the working

halves during Expedition 362, the Expedition 353 sampling party, or additional personal visits to Kochi Core Center using the standard plastic 10 cm<sup>3</sup> scoop and tube containers.

## 2.2. Laboratory preparation

Marine ash samples were disaggregated in an ultrasonic bath, if necessary, and subsequently wet-sieved into different grain size fractions (63–125, 125–250, >250, and, if necessary, 32–63 μm). The 63–125 μm fraction was further used for compositional analysis of glass shards with the electron microprobe (EMP) and laser ablation-inductively coupled plasma-mass spectrometer (LA-ICP-MS). Repeatedly, twelve different samples were embedded with two-component epoxy resin araldite into one 1 inch predrilled acrylic mount with twelve 2 mm holes. Afterward, the sample surfaces were polished (last polishing paste = 1 μm grain size) and the mounts were carbon coated to provide discharge of the electrons during EMP measurements.

## 2.3. Electron microprobe analyses

Glass shards (~5000 in total) were analyzed for major and minor elements on 310 epoxy embedded samples (15–30 shards per sample) using a JEOL JXA 8200 wavelength dispersive EMP at GEOMAR Helmholtz Center for Ocean Research Kiel utilizing the methods of Kutterolf et al. (2011). A calibrated measuring program was used based on international standards with a 6 nA strong and 10 μm large electron beam to minimize sodium loss. Oxide concentrations were determined using the ZAF correction method. Accuracy was monitored with two measurements each on Lipari obsidian (Lipari rhyolite) (Hunt and Hill, 2001) and Smithsonian basaltic standard VGA99 (Makaopuhi Lava Lake, Hawaii) (Jarosewich et al., 1980) after every 80 glass shard measurements. The 1σ standard deviations in comparison to reference values are <2% for major and <5% for minor elements (with the exception of P<sub>2</sub>O<sub>5</sub>, MgO, and MnO in Lipari and MnO in VGA99). All analyses with totals >90 wt% were normalized to 100% to eliminate the effects of variable postdepositional hydration and minor deviations of the electron beam. Analyses that show clear signs of microcrystal contamination (e.g., increased Al<sub>2</sub>O<sub>3</sub>, CaO, and Na<sub>2</sub>O for plagioclase and increased MgO and FeO<sub>t</sub> for olivine or pyroxene) were excluded. All of the resulting major and trace element data and their respective errors are listed in Tables S1, S2, and S3 in SAMPLES in [Supplementary material](#).

## 2.4. Laser ablation-inductively coupled plasma-mass spectrometry

The trace element concentrations of ~1000 glass shards from marine tephtras (214 samples; 3–6 shards per sample) were determined using LA-ICP-MS in December 2017, September 2018, and September 2020 at the Academia Sinica in Taipei, Taiwan. The LA-ICP-MS instrumentation comprises a 193 nm excimer laser (Teledyne CETAC Analyte G2) set to a spot size of 24–30 μm (energy density = 5–10 J/cm<sup>2</sup>; repetition rate = 4–10 Hz), coupled to a high-resolution inductively coupled plasma-mass spectrometer (ICP-MS) (Agilent 7900). Following 45 s of blank acquisition, typical ablation times were around 75 s. Data reduction was performed using “real-time on-line” GLITTER software (version 4.0) (Van Achterberg et al., 2001) immediately following each ablation analysis. Individual silica and calcium concentrations, measured using an EMP, mostly on the same glass shards, were used as an internal standard to calibrate each trace element analyses. An international glass standard from the USGS (BCR-2g; Wilson, 1997) was measured every 10 sample measurements to monitor accuracy and correct for matrix effects and signal drift in the ICP-MS as well as differences in the ablation efficiency between sample and reference material (Günther et al., 1999). The concentrations of NIST SRM 612, needed for external calibration, were taken from Norman et al. (1996) and Jochum et al. (2011). The limit of detection (LOD) for most trace elements was generally <100 ppb. For rare earth elements, the LOD is generally around 10 ppb. The 1σ analytical precision compared to standard reference data of BCR-2g is generally better than 5% for Li, Sc, Cr, Rb, Sr, Ba, La, Ce, Pr, Nd, Sm, Eu, Dy, Er, Lu, Hf, Pb, and U and better than 10% for the rest of the trace elements (Co, Zr, Nb, Cs, Gd, Tb, Ho, Tm, Yb, Ta, and Th), except for Y (12.5%) (see Table S3 in SAMPLES in [Supplementary material](#)).

### 3. Results

From 310 suspected ash-bearing samples from all investigated sites, 254 samples contained enough suitable fresh glass shards in the 63–125  $\mu\text{m}$  grain size fraction that were measurable for major and trace element compositions; the rest were too altered or were identified as turbidites. A total of 235 samples can be classified as primary tephra layers, containing pyroclasts as the predominant component in their clast inventory often exceeding 90 vol% in smear slides.

Taken as a whole, the analyzed glass shards of 254 ash-bearing horizons encompass basaltic to rhyolitic as well as trachytic compositions with rare basaltic trachyandesitic and trachyandesitic exceptions (Figure F2A), following the total alkali versus silica classification diagram after Le Maitre et al. (2002). The majority falls into the fields of rhyolite and trachyte as well as basalt and basaltic andesite. Apart from these major groups, all other samples straddle widely around intermediate andesitic, dacitic, trachyandesitic, and basaltic trachyandesitic compositions. Additionally, most of the glass shards are potassium rich and plot above the dividing line between normal and high-K calc-alkaline compositions, partly even crossing the shoshonitic composition dividing line (Figure F2B). Rare exceptions are potassium-poor glasses that plot below the calc-alkaline dividing line.

By evaluating trace element ratios, we compared the conducted glass compositions between arc-derived and ocean island–derived settings (e.g., ocean-island basalt =  $\text{Ba/La} < 20$  and  $\text{Nb/Rb} > 0.4$ ). Comparing all acquired data, it is obvious that the arc-derived glass shards, a majority presumably of Sunda arc origin, are limited to rhyolitic and rare dacitic and andesitic compositions (Figure F2A). They also follow a high-K or normal calc-alkaline trend with some exceptions that fall below the normal calc-alkaline magma series (Figure F2B). Based on the shipboard age models (McNeill et al., 2017b; Clemens et al., 2016; France-Lanord et al., 2016; Shipboard Scientific Party, 1974; Peirce et al., 1989; Cochran et al., 1989), the ages of the arc-related tephra layers range from the Oligocene to recent.

The measured glass shards that can preliminarily be associated to the different sampled submarine and subaerial ocean-island volcanoes in the Indian Ocean show a much broader compositional range than the arc-derived tephtras and cover all rock suites from basalt to rhyolite as well as basaltic trachyandesite to trachyte (Figure F2A). The compositions accumulate within the basalts and basaltic andesites of the calc-alkaline magmatic series as well as the intermediate to higher evolved rock suites (high-K dacite, high-k rhyolite, shoshonite, latite, and trachyte) of the high-K calc-

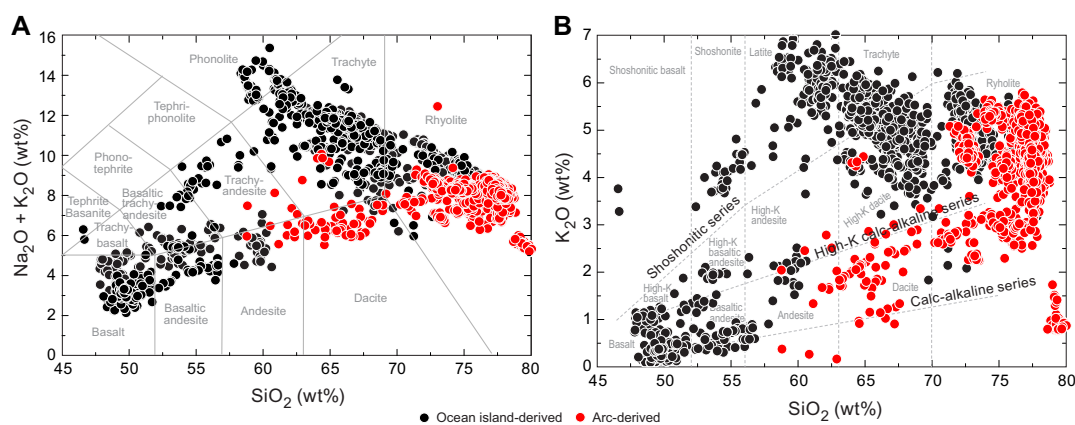


**Figure F2.** Glass-shard compositional ranges of marine tephtras sampled in 25 deep drilling sites of the Indian Ocean (normalized to 100 wt% anhydrous compositions). A. Total alkalis vs. silica diagram showing the volcanic rock classification after Le Maitre et al. (2002). Most samples follow a basaltic to rhyolitic trend. Note the separate trend of trachybasaltic to trachytic glass shards. Presumably arc-derived tephtras (red circles) are constrained to andesitic, dacitic, and rhyolitic compositions, whereas ocean island–derived tephtras (black circles) also contain more primitive and alkali-enriched compositions. B. Potassium vs. silica diagram showing the classifications after Peccerillo and Taylor (1976) into calc-alkaline, high-K calc-alkaline, and shoshonitic magmatic series. Presumably arc-derived tephtras are limited to the high-k and normal calc-alkaline magmatic series; ocean island–derived tephtras additionally fall into the shoshonitic magmatic series.

alkaline and shoshonite magmatic series (Figure **F2B**). Referring to the shipboard age models (Coffin et al., 2000; Peirce et al., 1989; Schlich et al., 1989; Barron et al., 1989; Backman et al., 1988), tephra layers from the Broken Ridge (Sites 752 and 753) represent the oldest measured glass shards and cover a narrow range from the middle Eocene to late Paleocene, whereas the investigated tephras from the Kerguelen Plateau (Sites 737, 747, and 1138; late Oligocene to Pleistocene) and the Seychelles region (Sites 706, 708, and 709; early Oligocene to Pleistocene) reveal glass compositions throughout the last 35 My.

## 4. Acknowledgments

This research used samples and data provided by IODP, ODP, and DSDP. The excellent efforts of all participating on- and offshore IODP technicians, laboratory and leading officers, Siem Offshore officers and crew, drilling personnel, and scientific parties are greatly acknowledged here; this report was made possible by their hard work. Funding for this research was provided by the German Research Foundation (DFG) within the DFG IODP Priority Programme (KU2685/10-1 and SCHI1349/4-1).

## References

- Backman, J., Duncan, R.A., et al., 1988. *Proceedings of the Ocean Drilling Program, Initial Reports*, 115: College Station, TX (Ocean Drilling Program). <https://doi.org/10.2973/odp.proc.ir.115.1988>
- Barron, J., Larsen, B., et al., 1989. *Proceedings of the Ocean Drilling Program, Initial Reports*, 119: College Station, TX (Ocean Drilling Program). <https://doi.org/10.2973/odp.proc.ir.119.1989>
- Clemens, S.C., Kuhnt, W., LeVay, L.J., Anand, P., Ando, T., Bartol, M., Bolton, C.T., Ding, X., Gariboldi, K., Giosan, L., Hathorne, E.C., Huang, Y., Jaiswal, P., Kim, S., Kirkpatrick, J.B., Littler, K., Marino, G., Martinez, P., Naik, D., Peketi, A., Phillips, S.C., Robinson, M.M., Romero, O.E., Sagar, N., Taladay, K.B., Taylor, S.N., Thirumalai, K., Uramoto, G., Usui, Y., Wang, J., Yamamoto, M., and Zhou, L., 2016. Expedition 353 summary. In Clemens, S.C., Kuhnt, W., LeVay, L.J., and the Expedition 353 Scientists, *Indian Monsoon Rainfall. Proceedings of the International Ocean Discovery Program, 353*: College Station, TX (Proceedings of the International Ocean Discovery Program). <https://doi.org/10.14379/iodp.proc.353.101.2016>
- Cochran, J.R., Stow, D.A.V., et al., 1989. *Proceedings of the Ocean Drilling Program, Initial Reports*, 116: College Station, TX (Ocean Drilling Program). <https://doi.org/10.2973/odp.proc.ir.116.1989>
- Coffin, M.F., Frey, F.A., Wallace, P.J., et al., 2000. *Proceedings of the Ocean Drilling Program, Initial Reports*, 183: College Station, TX (Ocean Drilling Program). <https://doi.org/10.2973/odp.proc.ir.183.2000>
- France-Lanord, C., Spiess, V., Klaus, A., Schwenk, T., Adhikari, R.R., Adhikari, S.K., Bahk, J.-J., Baxter, A.T., Cruz, J.W., Das, S.K., Dekens, P., Duleba, W., Fox, L.R., Galy, A., Galy, V., Ge, J., Gleason, J.D., Gyawali, B.R., Huyghe, P., Jia, G., Lantzsch, H., Manoj, M.C., Martos Martin, Y., Meynadier, L., Najman, Y.M.R., Nakajima, A., Ponton, C., Reilly, B.T., Rogers, K.G., Savian, J.F., Selkin, P.A., Weber, M.E., Williams, T., and Yoshida, K., 2016. Expedition 354 summary. In France-Lanord, C., Spiess, V., Klaus, A., Schwenk, T., and the Expedition 354 Scientists, *Bengal Fan. Proceedings of the International Ocean Discovery Program, 354*: College Station, TX (International Ocean Discovery Program). <https://doi.org/10.14379/iodp.proc.354.101.2016>
- Günther, D., Jackson, S.E., and Longerich, H.P., 1999. Laser ablation and arc/spark solid sample introduction into inductively coupled plasma mass spectrometers. *Spectrochimica Acta Part B: Atomic Spectroscopy*, 54(3–4):381–409. [https://doi.org/10.1016/S0584-8547\(99\)00011-7](https://doi.org/10.1016/S0584-8547(99)00011-7)
- Hunt, J.B., and Hill, P.G., 2001. Tephrological implications of beam size–sample-size effects in electron microprobe analysis of glass shards. *Journal of Quaternary Science*, 16(2):105–117. <https://doi.org/10.1002/jqs.571>
- Jarosewich, E., Nelen, J.A., and Norberg, J.A., 1980. Reference samples for electron microprobe analysis. *Geostandards Newsletter*, 4(1):43–47. <https://doi.org/10.1111/j.1751-908X.1980.tb00273.x>
- Jochum, K.P., Weis, U., Stoll, B., Kuzmin, D., Yang, Q., Raczek, I., Jacob, D.E., Stracke, A., Birbaum, K., Frick, D.A., Günther, D., and Enzweiler, J., 2011. Determination of reference values for NIST SRM 610–617 glasses following ISO guidelines. *Geostandards and Geoanalytical Research*, 35(4):397–429. <https://doi.org/10.1111/j.1751-908X.2011.00120.x>
- Kutterolf, S., Freundt, A., and Burkert, C., 2011. Eruptive history and magmatic evolution of the 1.9 kyr Plinian dacitic Chiltepe tephra from Apoyeque volcano in west-central Nicaragua. *Bulletin of Volcanology*, 73(7):811–831. <https://doi.org/10.1007/s00445-011-0457-0>
- Kutterolf, S., Schindlbeck-Belo, J., Pank, K., Wang, K.-L., and Lee, H.-Y., 2023. Supplementary material, <https://doi.org/10.14379/iodp.proc.362.207supp.2023>. In Kutterolf, S., Schindlbeck-Belo, J., Pank, K., Wang, K.-L., and Lee, H.-Y., 2023. Data report: chemical compositions of marine tephra layers in the Indian Ocean, IODP Expeditions 353 and 362. In McNeill, L.C., Dugan, B., Petronotis, K.E., and the Expedition 362 Scientists, *Sumatra Subduction Zone. Proceedings of the International Ocean Discovery Program, 362*: College Station, TX (International Ocean Discovery Program).
- Le Maitre, R.W., Streckeisen, A., Zanettin, B., Le Bas, M.J., Bonin, B., and Bateman, P., 2002. *Igneous Rocks: A Classification and Glossary of Terms: Recommendations of the International Union of Geological Sciences Subcommis-*

- sion on the Systematics of Igneous Rocks: Cambridge (Cambridge University Press).  
<https://doi.org/10.1017/CBO9780511535581>
- McNeill, L.C., Dugan, B., Backman, J., Pickering, K.T., Poudroux, H.F.A., Henstock, T.J., Petronotis, K.E., Carter, A., Chemale, F., Milliken, K.L., Kutterolf, S., Mukoyoshi, H., Chen, W., Kachovich, S., Mitchison, F.L., Bourlange, S., Colson, T.A., Frederik, M.C.G., Guèrin, G., Hamahashi, M., House, B.M., Hüpers, A., Jeppson, T.N., Kenigsberg, A.R., Kuranaga, M., Nair, N., Owari, S., Shan, Y., Song, I., Torres, M.E., Vannucchi, P., Vrolijk, P.J., Yang, T., Zhao, X., and Thomas, E., 2017a. Understanding Himalayan erosion and the significance of the Nicobar Fan. *Earth and Planetary Science Letters*, 475:134–142. <https://doi.org/10.1016/j.epsl.2017.07.019>
- McNeill, L.C., Dugan, B., Petronotis, K.E., Backman, J., Bourlange, S., Chemale, F., Jr., Wenhuang, C., Colson, T.A., Frederik, M.C.G., Guèrin, G., Hamahashi, M., Henstock, T., House, B.M., Hüpers, A., Jeppson, T.N., Kachovich, S., Kenigsberg, A.R., Kuranaga, M., Kutterolf, S., Milliken, K.L., Mitchison, F.L., Mukoyoshi, H., Nair, N., Owari, S., Pickering, K.T., Poudroux, H.F.A., Yehua, S., Song, I., Torres, M.E., Vannucchi, P., Vrolijk, P.J., Tao, Y., and Zhao, X., 2017b. Expedition 362 summary. In McNeill, L.C., Dugan, B., Petronotis, K.E., and the Expedition 362 Scientists, Sumatra Subduction Zone. *Proceedings of the International Ocean Discovery Program*, 362: College Station, TX (International Ocean Discovery Program). <https://doi.org/10.14379/iodp.proc.362.101.2017>
- McNeill, L.C., Dugan, B., Petronotis, K.E., Backman, J., Bourlange, S., Chemale, F., Chen, W., Colson, T.A., Frederik, M.C.G., Guèrin, G., Hamahashi, M., Henstock, T., House, B.M., Hüpers, A., Jeppson, T.N., Kachovich, S., Kenigsberg, A.R., Kuranaga, M., Kutterolf, S., Milliken, K.L., Mitchison, F.L., Mukoyoshi, H., Nair, N., Owari, S., Pickering, K.T., Poudroux, H.F.A., Yehua, S., Song, I., Torres, M.E., Vannucchi, P., Vrolijk, P.J., Yang, T., and Zhao, X., 2017c. Site U1480. In McNeill, L.C., Dugan, B., Petronotis, K.E., and the Expedition 362 Scientists, Sumatra Subduction Zone. *Proceedings of the International Ocean Discovery Program*, 362: College Station, TX (International Ocean Discovery Program). <https://doi.org/10.14379/iodp.proc.362.103.2017>
- McNeill, L.C., Dugan, B., Petronotis, K.E., Backman, J., Bourlange, S., Chemale, F., Chen, W., Colson, T.A., Frederik, M.C.G., Guèrin, G., Hamahashi, M., Henstock, T., House, B.M., Hüpers, A., Jeppson, T.N., Kachovich, S., Kenigsberg, A.R., Kuranaga, M., Kutterolf, S., Milliken, K.L., Mitchison, F.L., Mukoyoshi, H., Nair, N., Owari, S., Pickering, K.T., Poudroux, H.F.A., Yehua, S., Song, I., Torres, M.E., Vannucchi, P., Vrolijk, P.J., Yang, T., and Zhao, X., 2017d. Site U1481. In McNeill, L.C., Dugan, B., Petronotis, K.E., and the Expedition 362 Scientists, Sumatra Subduction Zone. *Proceedings of the International Ocean Discovery Program*, 362: College Station, TX (International Ocean Discovery Program). <https://doi.org/10.14379/iodp.proc.362.104.2017>
- Norman, M.D., Pearson, N.J., Sharma, A., and Griffin, W.L., 1996. Quantitative analysis of trace elements in geological materials by laser ablation ICPMS: instrumental operating conditions and calibration values of NIST glasses. *Geo-standards Newsletter*, 20(2):247–261. <https://doi.org/10.1111/j.1751-908X.1996.tb00186.x>
- Peccerillo, A., and Taylor, S.R., 1976. Geochemistry of Eocene calc-alkaline volcanic rocks from the Kastamonu area, northern Turkey. *Contributions to Mineralogy and Petrology*, 58(1):63–81. <https://doi.org/10.1007/BF00384745>
- Peirce, J., Weissel, J., et al., 1989. *Proceedings of Ocean Drilling Program, Initial Reports: College Station, TX (Ocean Drilling Program)*. <https://doi.org/10.2973/odp.proc.ir.121.1989>
- Pickering, K.T., Poudroux, H., McNeill, L.C., Backman, J., Chemale, F., Kutterolf, S., Milliken, K.L., Mukoyoshi, H., Henstock, T.J., Stevens, D.E., Parnell, C., and Dugan, B., 2020. Sedimentology, stratigraphy and architecture of the Nicobar Fan (Bengal-Nicobar fan system), Indian Ocean; results from International Ocean Discovery Program Expedition 362. *Sedimentology*, 67(5):2248–2284. <https://doi.org/10.1111/sed.12701>
- Ryan, W.B.F., Carbotte, S.M., Coplan, J.O., O'Hara, S., Melkonian, A., Arko, R., Weissel, R.A., Ferrini, V., Goodwillie, A., Nitsche, F., Bonczkowski, J., and Zemsky, R., 2009. Global multi-resolution topography synthesis. *Geochemistry, Geophysics, Geosystems*, 10(3):Q03014. <https://doi.org/10.1029/2008GC002332>
- Schlich, R., Wise, S.W., Jr., et al., 1989. *Proceedings of the Ocean Drilling Program Initial Reports*, 120: College Station, TX (Ocean Drilling Program). <https://doi.org/10.2973/odp.proc.ir.120.1989>
- Shipboard Scientific Party, 1974. Introduction and explanatory notes. In von der Borch, C.C., Sclater, J.G., et al., *Initial Reports of the Deep Sea Drilling Project*. 22: Washington, DC (US Government Printing Office). <https://doi.org/10.2973/dsdp.proc.22.101.1974>
- Van Achterberg, E., Ryan, C., Jackson, S., and Griffin, W., 2001. Data reduction software for LA-ICP-MS. In Sylvester, P.J., *Laser Ablation ICP-MS in the Earth Sciences: Principles and Applications*. Mineralogical Association of Canada Short Course Series, 29: 239–243.
- Wilson, S.A., 1997. The collection, preparation and testing of USGS reference material BCR-2, Columbia River, basalt. *US Geological Survey Open-File Report*, 98-00x.